

## polymer papers

**Analysis of poorly crystallized polymers  
using resolution enhanced X-ray diffraction  
scans****N. S. Murthy\* and H. Minor***Research and Technology, AlliedSignal Inc., Morristown, NJ 07962, USA**(Received 25 August 1994)*

The use of resolution enhanced X-ray diffraction scans for studying small differences in the structures in poorly crystallized semicrystalline polymers is illustrated with examples from three polymers with different crystallization behaviour, namely nylon 6,6, nylon 6 and poly(chlorotrifluoro ethylene). The effects of small coherence length were deconvolved using maximum entropy methods to obtain clearly resolved peaks. In polymers such as nylon 6,6, the crystalline structure at low levels of crystallinity can be regarded as highly disordered ('paracrystalline') forms of the structures present in highly crystalline samples. In polymers such as nylon 6, it is necessary to identify the presence of less stable crystalline phases. Finally, in some instances, such as in rapidly quenched films of poly(chlorotrifluoro ethylene), transient crystalline phases could be present during initial phases of crystal growth. Coexistence of the crystalline phases, transient crystalline phases and the amorphous phase are discussed.

(Keywords: X-ray diffraction; structure; semicrystalline polymers)

**INTRODUCTION**

The crystalline regions in many semicrystalline polymers at certain stages during processing are highly disordered, and the features of the three-dimensional crystalline order cannot be readily identified. Polymers in these states are not truly amorphous, but their crystallinities are hard to determine. Characterization of these types of polymers is of considerable practical utility, for example in assessing the suitability of these materials in thermoforming applications. Such materials are compliant, but are sufficiently dimensionally stable and do not age severely. A combination of these properties is not present in polymers which are either fully amorphous or possess a significant level of crystallinity. It is often difficult to characterize and quantify the structure during the transition from an amorphous to a stable crystalline phase. Such analysis is, however, necessary so that the effect of changes in processing parameters can be monitored. We address here the issue of the nature of the crystals in poorly crystallized semicrystalline polymers using data from three semicrystalline polymers: poly(chlorotrifluoro ethylene) (PCTFE), nylon 6 (N6) and nylon 6,6 (N66). These polymers were selected to illustrate our methods because of the different characteristics exhibited by these polymers at low levels of crystallinity.

**EXPERIMENTAL**

Poorly crystallized N66 films (thickness  $\sim 50 \mu\text{m}$ ) were

obtained by compression moulding Zytel 101 resin (DuPont) and rapidly quenching the film in ice/water. The films are almost amorphous immediately after quenching, and gradually crystallize upon exposure to ambient conditions. Slightly higher crystalline order was induced by immersing the film in a column of monochlorobenzene and orthodichlorobenzene used for density measurements. Highest crystallinity N66 film was obtained by moulding the film at  $245^\circ\text{C}$  for 15 h under positive pressure. The N6 films (thickness  $\sim 25 \mu\text{m}$ ) used in this analysis are commercial grade films (Capran 77A) produced by AlliedSignal Inc. These films are cast on a chilled roll, and hence have very low crystalline order. The crystalline order in the film was increased by annealing the film at  $190^\circ\text{C}$  for 1 h under dynamic vacuum. For comparison, a highly crystalline resin (BST-D), which contained both  $\alpha$  and  $\gamma$  crystalline form, was included. PCTFE films (thickness  $\sim 20 \mu\text{m}$ ) used in this study contain 3.5% of vinylidene fluoride as a comonomer, and are sold as Aclar (88A) by AlliedSignal Inc. These films are cast on cold rolls so as to inhibit the crystallization of the polymer. Films of increasing crystalline order were obtained by annealing the films at 80, 100 and  $170^\circ\text{C}$ . PCTFE film of highest crystallinity was obtained by casting a much thicker film at a higher casting temperature. A film of similar crystallinity (70%) but smaller crystallite size (100 Å compared to 400 Å) was prepared by quenching this film and then annealing it at  $160^\circ\text{C}$  for 6 h.

Flat-plate X-ray diffraction (XRD) photographs showed these samples to be essentially unoriented. XRD scans were obtained on a Philips powder diffractometer in parafocus geometry using  $\text{CuK}\alpha$

\*To whom correspondence should be addressed

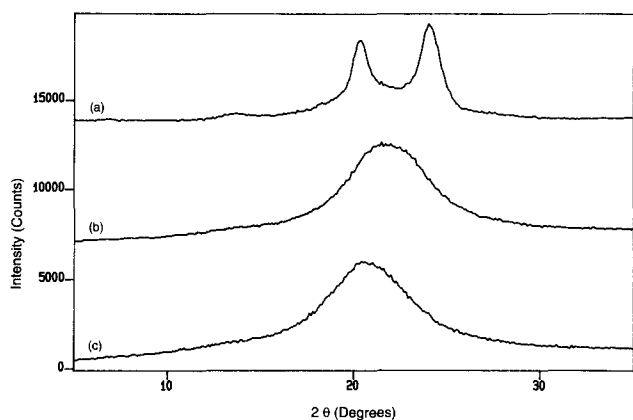


**Figure 1** XRD scans of (a) high crystallinity (46%) and (b), (c) low crystallinity (10–20%) N66 films

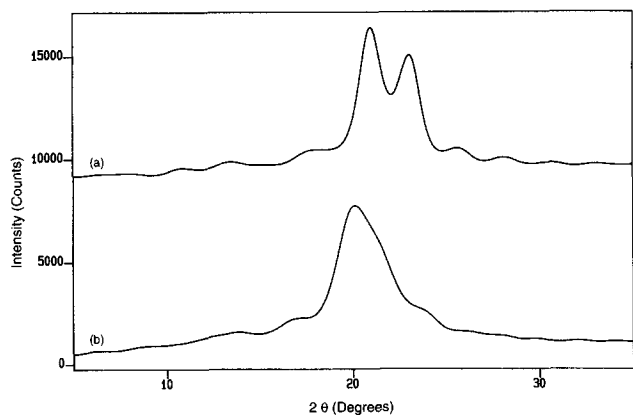


**Figure 2** XRD scans of poorly crystallized N66 deconvolved using a peak width of  $3^\circ$ . Curves (a) and (b) correspond to scans (b) and (c) in Figure 1

radiation from a sealed copper tube operated at 40 kV and 40 mA. The data were collected in steps of  $0.1^\circ/2$  s for N6 and N66, and  $0.02^\circ/20$  s for PCTFE. Additional PCTFE scans to determine the effect of noise on the deconvolution procedures were made on smaller samples and by counting for 1, 5 and 10 s.

The XRD scans are usually analysed by curve-fitting the data to crystalline and amorphous peaks in order to obtain crystallinity and crystallite sizes. However, in scans in which the peaks are poorly resolved, the results of least-squares analysis are dependent on the initial parameters, i.e. the number of peaks and their positions, widths and heights. To overcome this uncertainty, we propose here the use of resolution enhanced XRD scans to determine the number and position of the peaks prior to curve-fitting<sup>1</sup>. The XRD scans were sharpened by deconvolving the effect of broadening due to size and limited coherence. The scans were deconvolved using the program RAZOR (Spectrum Square Associates, Inc.) for GRAMS/386TM which picks the optimum solution using maximum entropy methods.

## RESULTS

XRD scans of two quenched N66 films, and a scan from highly crystalline N66 film are shown in Figure 1. Scans (b) and (c) appear to be very similar and essentially

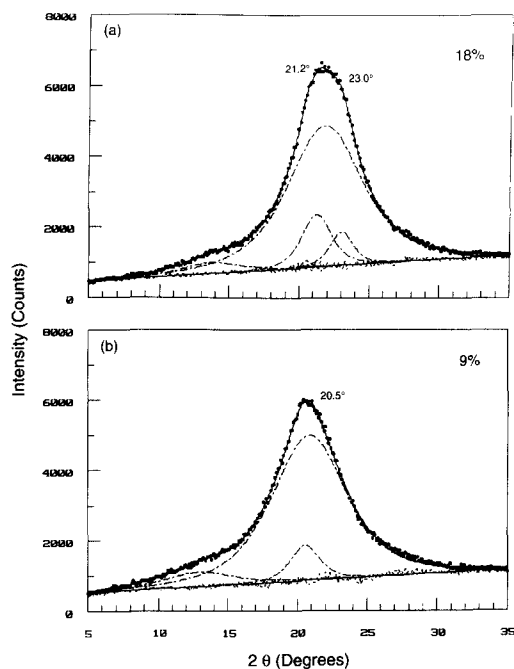


**Figure 3** Profile-fitted XRD scans of low crystallinity N66 films. (a) and (b) correspond to scans (b) and (c) in Figure 1. In these and other profile-fitted curves, the circles are the observed data, the line through the circles is the fitted curve, which is the sum of the components shown by dotted lines; the difference between the observed and the calculated intensities is shown as a dotted line oscillating about the base line which is drawn as a full line

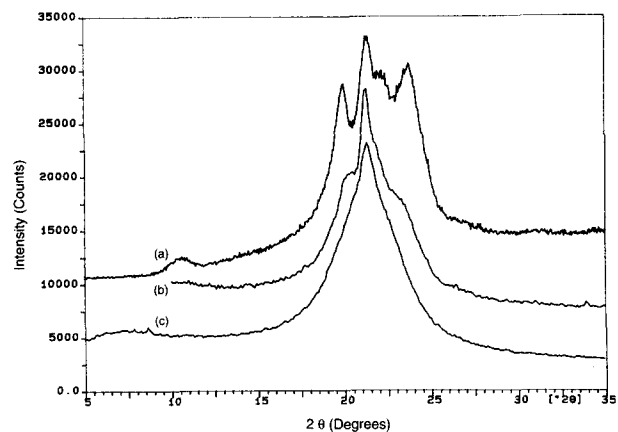


**Figure 4** XRD scans of N6 films with (a) high degree of crystalline order (45%) and (b), (c) low degree of crystalline order

amorphous. These scans were deconvolved with a peak width of  $3^\circ$  to enhance the differences between the two scans (Figure 2). Contrary to initial expectation, the deconvolved results show that the two featureless scans have different levels of crystalline order. The raw data from the 'amorphous' films were fitted on the basis of these deconvolved results (Figure 3). The scan in Figure 3a is due to the poorly ordered  $\alpha$  crystals<sup>2</sup>. The single crystalline peak in Figure 3b is not resolved even in the resolution enhanced scan, and shows that at low levels of crystallinity, the two crystalline peaks ( $21^\circ$  and  $23^\circ$ , seen in Figure 3a) merge into one.

XRD scans from poorly crystallized (as-cast) and annealed ( $190^\circ\text{C}$  for 1 h) N6 films are shown in Figure 4, together with a scan in which the various crystalline

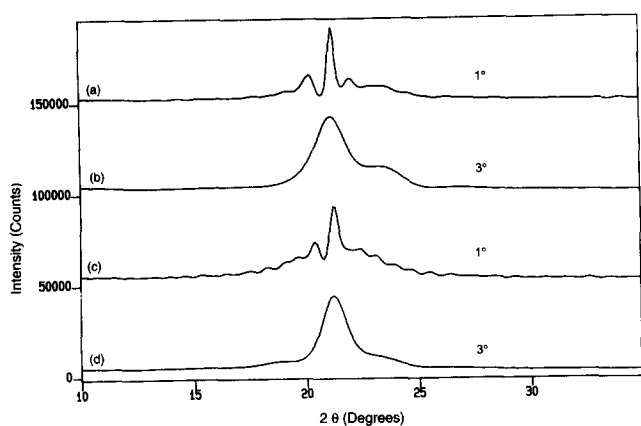


**Figure 5** Deconvolved XRD scans of poorly crystallized N6. Curves (a), (b) and (c), (d) are from scans (b) and (c), respectively, in Figure 4. Results obtained using peak widths of 1° ((a) and (c)) and 3° ((b) and (d)) are shown in the figure for comparison

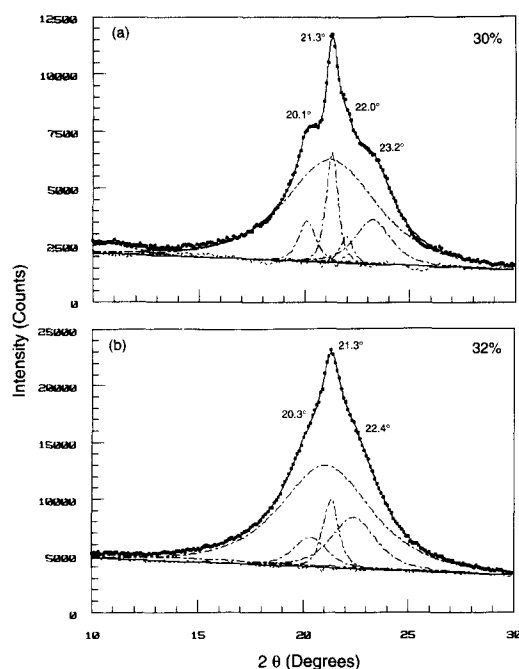


**Figure 6** Profile-fitted XRD scans of poorly crystallized N6. (a) and (b) correspond to scans (b) and (c) in Figure 4. See Figure 3 for explanation of curves

peaks are well resolved. Scans (b) and (c), from less crystalline samples, were deconvolved using a peak width of 1°. The results, given in Figure 5 (curves (a) and (c)), show that the two samples are similar except for the degree of crystalline order. Curves (b) and (d) in Figure 5 show that the crystalline features cannot be seen in scans deconvolved using a larger width (3°) for the peak broadening function. The results of deconvolution were used to curve-fit the scans (Figure 6). The peaks at 20° and 23° are from the thermodynamically stable  $\alpha$  crystalline form<sup>3</sup>, and those at 21° and 22° are from the less stable  $\gamma$  crystalline form<sup>4</sup>. The results show that annealing increases the crystallite size without increasing the total crystallinity.

The XRD scans from poorly crystallized PCTFE films of varying crystallinities are shown in Figure 7. The intense broad band at 39° is independent of the

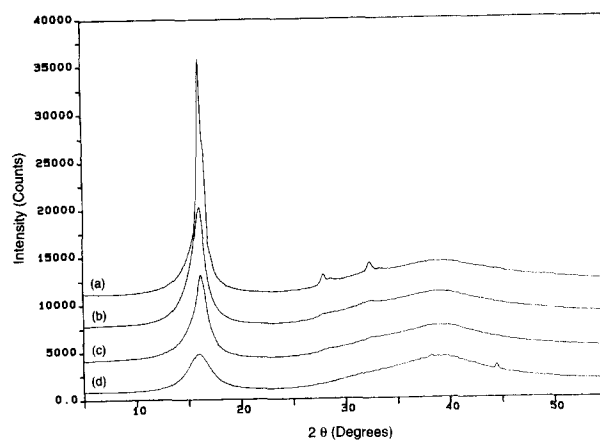


**Figure 7** XRD scans of PCTFE films of low but different crystallinities (see Figure 9). Annealing temperatures (and crystallinities) are: (a) 170°C (45%); (b) 100°C (35%); (c) 80°C (32%); (d) as received (9%)

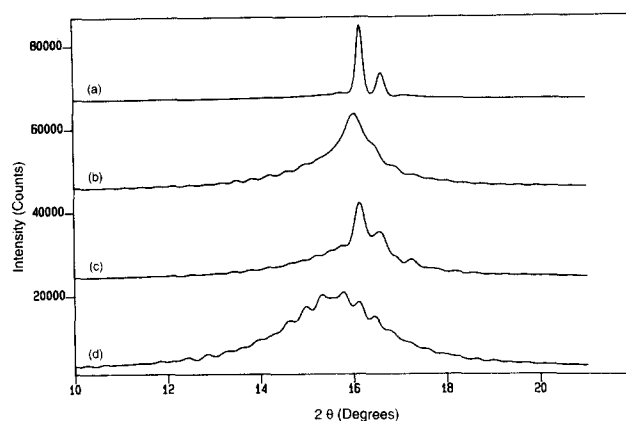


**Figure 8** XRD scans of PCTFE deconvolved for the line broadening using a 0.5° peak width. Curves (a)–(d) as in Figure 7

crystalline order, and therefore the intensity of this peak can be taken as a measure of total mass of the polymer<sup>5</sup>. The peak at 16° is sensitive to crystalline order. Thus, the different ratios of the 16° peak to the 39° band in the scans in Figure 7 show that the four scans represent three levels of crystallinity in the PCTFE films ((a) > (b) ~ (c) > (d)). The deconvolved scans (Figure 8; peak width = 0.5°) enhance the difference between scans (b) and (c) in Figure 7: scan (b) in Figure 8 shows only one crystalline peak and scan (c) (Figure 8) shows an additional weak, crystalline reflection. The deconvolution results were used to profile-fit the raw data (Figure 9). The crystalline peaks are indexed in the scan of a highly crystalline film in Figure 10a. The 16.3°, 16.7° and 17.2° peaks are, respectively, the (101), (102) and (103) reflections ( $c$  is the chain axis)<sup>6</sup>. The scans in Figures 9b and d, which do not show the (102) and (103) reflections, are from films in which there is no long order along the chain axis in the crystalline domains. Although the crystallinity of the films in Figure 9c is lower than that used for Figure 9b, chain-axis order, as evidenced by the presence of (102) and (103) reflections, is present only in Figure 9c. An extreme example is shown in Figure 10b, which is a scan from a highly crystalline film (70%), but unlike the scan in Figure 10a, does not show chain-axis order.

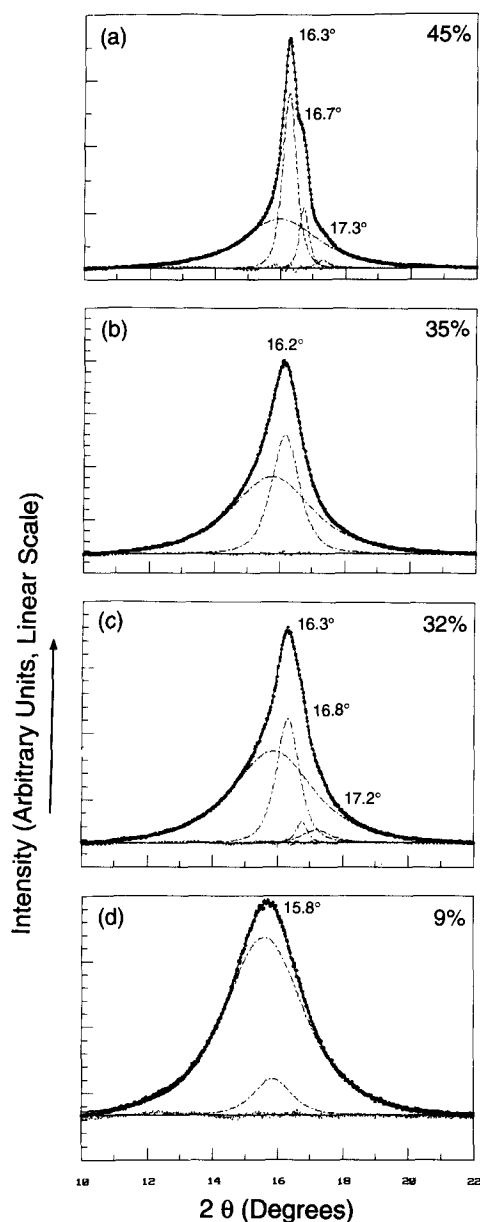


**Figure 9** Profile-fitted PCTFE scans. See Figure 3 for explanation of curves. Curves (a)–(d) as in Figure 7

## DISCUSSION

The data from the three polymers used in this study are usually interpreted in terms of the standard two-phase model in which the crystalline domains are embedded in a continuous amorphous matrix<sup>7</sup>. These polymers were chosen for two reasons. First, they exhibit different crystallization behaviour: N66 crystallizes in only crystalline form ( $\alpha$ ) and crystallizes faster than N6; N6 crystallizes in two crystalline forms,  $\alpha$  during slow crystallization rates and  $\gamma$  during faster crystallization; PCTFE crystallizes at about the same rate as N66, but the eventual crystallinity can be very high ( $\sim 80\%$  compared to  $\sim 50\%$  for nylons), and the structure of PCTFE at low levels of crystallinity ( $< 35\%$ ) is not clearly understood. Second, in analysing the poorly crystallized specimens of these three polymers for more than 20 years, we have found it difficult to use the current methods to quantify the small differences which are apparent in the raw data; these reproducible differences

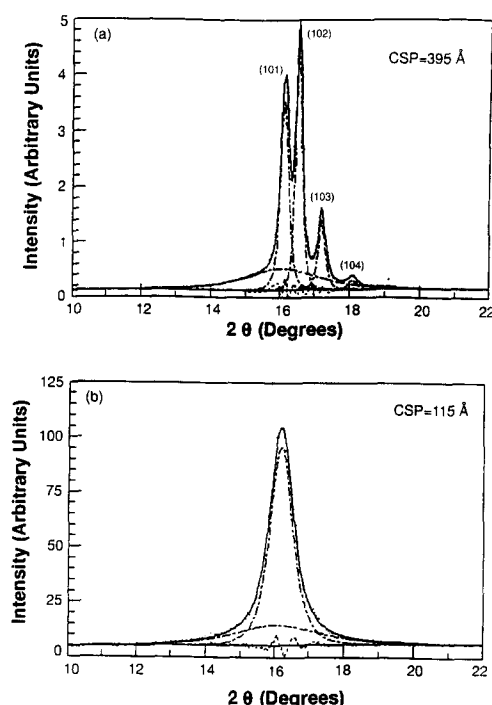


**Figure 10** Profile-fitted scans of two PCTFE films with (a) a high degree and (b) a low degree of chain-axis order. See Figure 3 for explanation of curves

are due to the known variations in processing parameters and result in marked differences in the performance of these materials. Our goal here is to characterize the differences within the crystalline phase in poorly crystallized samples. Typical analysis based on curve-fitting can be ambiguous because the final solution is very dependent on the choice of the starting parameters<sup>8</sup>. Sharpening of scans by deconvolving the effect of the limited coherence length is proposed here as one solution to limit the number of choices during curve-fitting of the data.

The shape and the width of the peak representing the broadening function need to be chosen prior to deconvolution. The peak shapes were deduced to be modified Lorentzians in the angular range of interest from the scans of inorganic standards, highly crystalline samples, and appeared to be not as important as the peak width. This is illustrated in Figure 11a. But the peak widths could not be ascertained beforehand. Too small a width does not enhance the resolution, and too large a width is meaningless and results in spurious peaks. This was discussed in our earlier paper<sup>1</sup>, and is further illustrated in Figure 11b. The solution is not straightforward because the coherence lengths of the various peaks in a scan are not necessarily the same, and the deconvolution method can be used to remove the broadening only from a single crystallite size distribution. The amorphous domains, which typically have a coherence length of  $\sim 20$  Å, need to be represented by a peak of width  $3$ – $6^\circ$ , and the crystalline domains with sizes  $> 30$  Å require peaks of widths  $0.2$ – $1.0^\circ$ . In this paper we are dealing with poorly crystallized samples in which only small crystallites are present. The sizes of these small crystallites depend on the polymer. The smallest size is typically  $60$  Å for PCTFE and  $25$  Å for polyamides, corresponding to widths of  $1.5^\circ$  and  $3^\circ$ ,

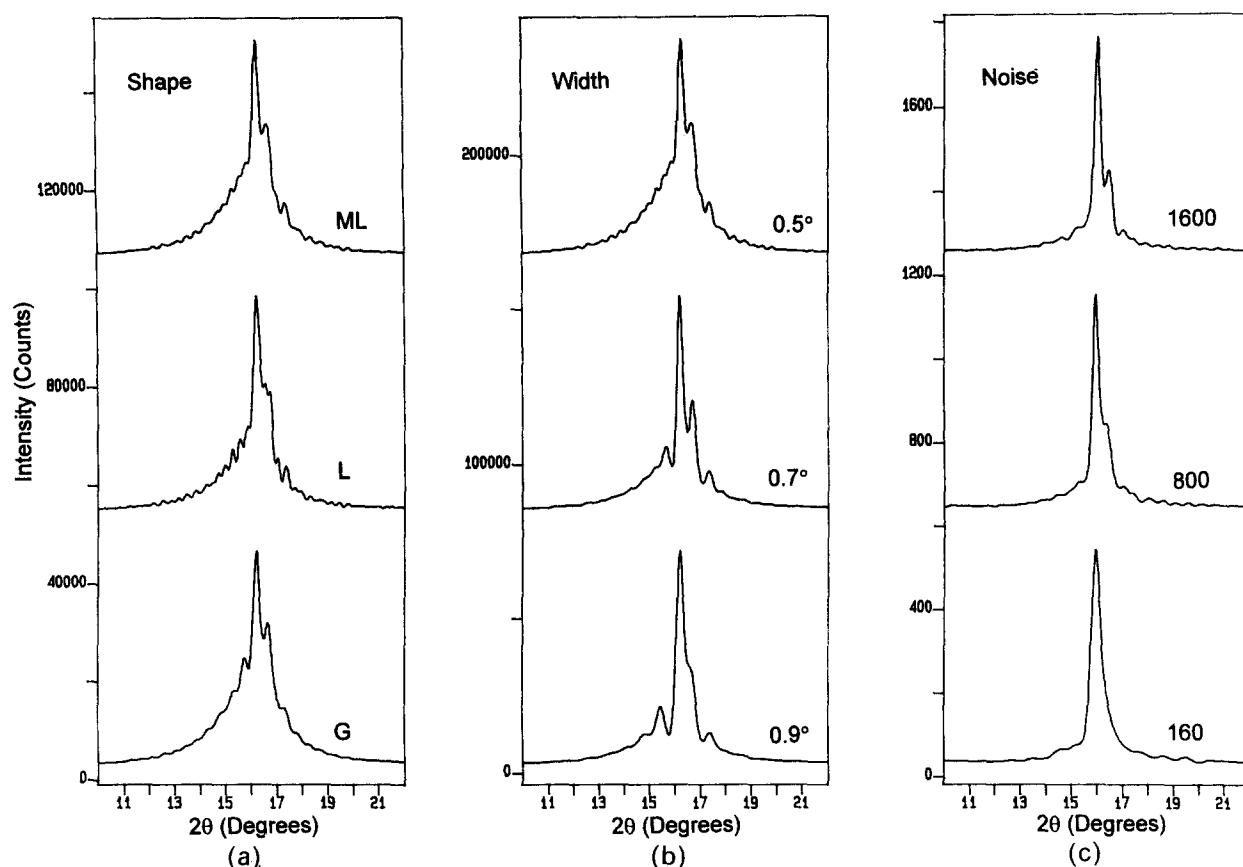


**Figure 11** Illustrations of the effects of peak shape, peak width and counting statistics on the deconvolved results. A PCTFE sample used in *Figure 7*, scan (c) is used for these data. (a) Three commonly used peak shapes (ML, modified Lorentzian; L, Lorentzian; G, Gaussian) give very similar results. (b) Whereas a peak width of  $0.5^\circ$  (size  $\sim 150$  Å) enhances the crystalline features, larger peak widths ( $0.7^\circ$  and  $0.9^\circ$ ) give rise to spurious peaks. Peaks much smaller than  $0.5^\circ$  enhance the random noise in the data<sup>1</sup>. (c) The crystalline features in the deconvolved results from data with a peak count of 1600 are similar to that with 36 000 counts seen in *Figure 8c*. However, much smaller peak counts of 800 and 160 fail to reproduce the crystalline features in the data

respectively. The largest observed sizes are typically 400 Å ( $0.2^\circ$ ) for PCTFE and 150 Å ( $0.5^\circ$ ) for nylons. As a result of several trials based on these considerations, peak widths between  $0.2^\circ$  and  $1.5^\circ$  were used for deconvolving PCTFE scans, while peak widths of  $0.5$ – $3^\circ$  were used for nylons. Although the maximum entropy method can be used to enhance the data with poor counting statistics, the method fails in extreme cases, as illustrated in *Figure 11c*. However, the method can be successful in most routine analysis with data obtained at 4 s/step using a sealed tube. In contrast, other deconvolution methods, such as Fourier analysis, require data with extremely good counting statistics collected for times of 10–100 times longer<sup>1</sup>.

Many crystallizable polymers can be obtained not in a truly amorphous state but in a 'mostly' amorphous state. Scans such as those in *Figure 1(b)* and (c), for N66 and *Figure 7(b)* and (c), for PCTFE appear to be from amorphous samples. But the width of the diffuse peak is smaller, the position is shifted to slightly higher angles, and the peak is more asymmetric than that seen in a melt or a rapidly quenched sample. Furthermore, the resolution enhanced scans show that crystalline features are indeed present in these scans. Although the coherence lengths corresponding to these peaks are small, they have to be regarded as crystalline and not amorphous peaks. The data from N66 in *Figures 2* and *3* show that such crystalline peaks are not resolved because, in addition to low crystallinities in these films, the crystals are small,

disordered, or both. But the structures in these crystals are similar to those present in highly crystalline polymers. Although the possibility of a metastable phase in N6 cannot be ruled out<sup>9,10</sup>, the scans shown in *Figure 6* show essentially poorly crystallized forms of  $\alpha$  or  $\gamma$  crystals<sup>11,12</sup>. Increase in crystallinity is usually accompanied by an increase in crystalline order within the crystalline domains and increase in the crystallite size.

In some instances, a new structure, whose diffraction pattern is different from that in a highly crystalline sample, could be present. We will discuss one such example using the data from PCTFE. The main (101) reflection in *Figures 9b* and *c* occurs at a lower angle and is broad, indicating the presence of larger unit cells and relatively small, highly disordered crystallites. The absence of higher order reflections ((102), (103) and (104)) indicates that there is no long-range order along the chain axis. As the crystallite size increases, the chain-axis order also increases, and the (102), (103) and (104) reflections appear (*Figures 9a* and *c*). However, the relative intensities of these reflections are different from those in highly crystalline film (*Figure 10a*). More importantly, the width of the (101) peak is larger than that of (102). If the (101) and (102) reflections are from the same crystalline domains, (101) should be sharper than (102). Thus, the main peak in *Figure 9c* is a composite of two reflections: a peak of the type in *Figure 10a* from crystals with a high degree of chain-axis order,

and a second peak of the type in Figure 10b from crystals with poor chain-axis order. The latter type of crystal could be similar to that observed by Miyamoto *et al.* in high-pressure crystallized PCTFE<sup>13</sup>. This suggests that as the crystalline order of PCTFE increases, at crystallinities between 30 and 40%, a fraction of the quasi-ordered crystals transforms into highly ordered crystals, and these new highly ordered crystals coexist with the quasi-ordered precursors and the amorphous phase. A similar situation could exist in other polymers as well.

The paracrystalline phase of Hosemann and Bagchi<sup>14</sup> perhaps best describes the poorly ordered phases being discussed here. Although this term is often used to describe structures which are not quite crystalline but are not truly amorphous, it strictly refers to structures with a specific kind of crystalline disorder, the disorder of the second kind. The poorly ordered phases cannot be described as pseudohexagonal, a term which refers to a structure in which molecules are in a hexagonal lattice, but their orientations do not have a six-fold symmetry. Some of the poorly ordered structures have been found to be metastable<sup>9,10</sup>. There are also polymers which exhibit distinctly new phases when poorly crystallized. Smectic-like ordering in drawn poly(ethylene terephthalate) is one recent example<sup>15</sup>. In many instances it is necessary to distinguish these intermediate structures from the small, disordered forms of the stable three-dimensional crystals. Therefore, we will refer to these intermediate, quasi-ordered, paracrystalline, metastable, liquid-crystalline phases as transient crystalline phases to emphasize their crystalline nature and their propensity to change. Thus, we have an amorphous phase, a transient crystalline phase and a crystalline phase. Identification and stabilization of such transient crystalline phases can provide a means for engineering the desired properties in a polymer<sup>16</sup>.

Wunderlich and co-workers have recently invoked an intermediate phase, in addition to the amorphous and crystalline phases, to interpret fibre diffraction results<sup>17,18</sup>. They attribute the intensity remaining after subtracting the crystalline and the isotropic amorphous intensity from the observed intensity to this intermediate phase. In our previous work<sup>19,20</sup>, we have referred to this intermediate phase as the anisotropic amorphous component to emphasize the common origin of the isotropic and anisotropic diffuse scattering. In contrast to this intermediate phase or the anisotropic component,

the transient crystalline phase gives rise to crystalline-like reflections rather than diffuse scattering, and orientation is not a prerequisite to its formation.

## CONCLUSIONS

In many polymers, such as N6 and N66, the structure within small, disordered crystallites is not different from that in highly crystalline samples. Transient crystalline phases can be identified in some polymers, such as PCTFE, and these phases coexist with more stable, highly ordered crystallites over a limited range of crystallinities.

## REFERENCES

- 1 Murthy, N. S., Zero, K. and Minor, H. *Macromolecules* 1994, **27**, 1484
- 2 Bunn, C. W. and Garner, E. V. *Proc. R. Soc. (London)* 1947, **A189**, 39
- 3 Holmes, D. R., Bunn, C. W. and Smith, D. J. *J. Polym. Sci.* 1955, **17**, 159
- 4 Arimoto, H., Ishibashi, M., Hirai, M. and Chatani, Y. *J. Polym. Sci. Part A* 1965, **3**, 317
- 5 Roldan, L. G. and Kaufman, H. S. *Norelco Reporter* 1963, **10**, 11
- 6 Mencik, Z. *J. Polym. Sci., Polym. Phys. Edn.* 1973, **11**, 1585
- 7 Baltá-Calleja, F. J. and Vouk, C. J. 'X-ray Scattering of Synthetic Polymers', Elsevier, Amsterdam, 1989, p. 175
- 8 Murthy, N. S. and Minor, H. *Polymer* 1990, **31**, 996
- 9 Murthy, N. S. and Minor, H. *Polym. Commun.* 1991, **32**, 297
- 10 Murthy, N. S. *Polym. Commun.* 1991, **32**, 301
- 11 Parker, J. P. and Lindenmayer, P. H. *J. Appl. Polym. Sci.* 1971, **21**, 821
- 12 Gianchandani, J., Spruiell, J. E. and Clark, E. S. *J. Appl. Polym. Sci.* 1982, **27**, 3527
- 13 Miyamoto, Y., Nakafuku, C. and Takemura, T. *Polym. J.* 1972, **3**, 122
- 14 Hosemann, R. and Bagchi, S. N. 'Direct Analysis of Diffraction by Matter', North-Holland, Amsterdam, 1962
- 15 Auriemma, F., Corradini, P., De Rosa, C., Guerra, G., Petraccone, V., Bianchi, R. and Di Dino, G. *Macromolecules* 1992, **25**, 2490
- 16 Davey, R. J., Maginn, S. J., Andrews, S. J., Buckley, A. M., Cotter, D., Dempsey, P., Rout, J. E., Stanley, D. R. and Taylor, A. *Nature* 1993, **366**, 248
- 17 Fu, Y., Busing, W. R., Jin, Y., Affholter, K. A. and Wunderlich, B. *Macromol. Chem.* 1994, **195**, 803
- 18 Fu, Y., Annis, B., Boller, A., Jin, Y. and Wunderlich, B. *J. Polym. Sci., Polym. Phys. Edn* 1994, **32**, 2289
- 19 Murthy, N. S., Correale, S. T. and Moore, R. A. F. *J. Appl. Polym. Sci., Appl. Polym. Symp.* 1991, **47**, 185
- 20 Murthy, N. S., Minor, H., Bednarczyk, C. and Krimm, S. *Macromolecules* 1993, **26**, 1712